International Journal of Mining and Geo-Engineering

IJMGE

IJMGE 53-1 (2019) 25-31

DOI: 10.22059/ijmge.2018.256299.594732

Determination of the difference in recovery and kinetics of various size fractions of gilsonite in rougher and cleaner flotation processes

Fatemeh Kazemi [a], Ataallah Bahrami [a, *], Jafar Abdolahi Sharif [a]

[a] *Department of Mining Engineering, Faculty of Engineering, Urmia University, Urmia, Iran*

Article History:

Received: 21 April 2018,

Revised: 24 July 2018,

Accepted: 27 September 2018.

ABSTRACT

Kinetic models are the most important tools for the prediction and evaluation of the flotation circuits performance. In order to determine the kinetic order and rate of flotation of a Gilsonite sample, flotation experiments were conducted using the combination of Gasoline-Pine Oil, and one test without any collector and frother. The pulp density was 10% and the experiments were carried out in both rougher and cleaner stages using different size fractions. Five first order kinetic models were applied to the data obtained from the flotation tests by using the Matrix Laboratory software. Statistical analysis demonstrated that the results of Gasoline-Pine Oil experiment have a high degree of compliance with the all models. Rougher and cleaner tests without collector and frother also matched with the modified gas/solid adsorption and rectangular models with the k values of 0.0869 (s^{-1}), and 0.0266 (s^{-1}), respectively. The relationship between flotation rate constant, maximum combustible recovery and particle size were also studied. The results showed that the maximum flotation combustible recovery and flotation rate were obtained with an intermediate particle size in the rougher flotation processes. The maximum combustible recovery and flotation rate in the cleaner flotation process was related to the particle size categories of -850+500 (μm) and -500+250 (μm), respectively.

Keywords : *Rate of flotation; Kinetic models; Gilsonite; Combustible recovery, Particle size*

1. Introduction

In order to effectively estimate, predict, and evaluate the performance of flotation circuits, different models have been presented. Among them, kinetic models can be implemented to determine the optimized residence time, design the circuits, and control the systems. It is also used in optimization of the type and determination of the concentration of chemicals and other fundamental parameters [1].

The flotation operation and its associated kinetics and thermodynamics are somewhat arbitrary phenomena [2]. The number of particles that permanently stick to the bubble surface, results in that the recovery to be time-dependent. Various kinetic models are suggested to explain flotation recovery from different aspects. Therefore, the models are complementary to each other. The initial batch flotation model was reported by Garcia-Zuniga (1935) [3]. He applied the differential equation of kinetics of chemical reaction to describe the process of batch flotation. The general form of the model can be written as:

$$\frac{dc(t)}{dt} = -kc^n \quad (1)$$

The above equation was suggested by Arbiter (1951) for the experimental and industrial data in which C denotes the concentration of particles, t for time, k for flotation rate constant, and n is the kinetic order [4]. Imaizumi and Inoue put forward a new flotation model in which the flotation rate is a continuous distribution of the flotation rates of heterogeneous materials in the cell [5]. Lynch et al. (1981) showed that some of the kinetic models did not fit well with experimental data as some of the minerals float faster than the others [6].

The overall kinetic equation regarding the first and second order flotation kinetic is [7]:

$$k^i t = \frac{\frac{R^i}{R^i_\infty}}{1-\left(\frac{R^i}{R^i_\infty}\right)}\left(1-\frac{R^i_\infty}{R_\infty}\right) - \left(\frac{R^i_\infty}{R_\infty}\right) Ln\left(1-\frac{R^i}{R^i_\infty}\right) \quad (2)$$

In which, R is recovery at the time t, and R_∞ detones the combustible recovery. If just one mineral floats in the cell or pulp is dilute, then: $R^i_\infty = R_\infty$, but if the mineral is low in grade or the pulp density is high, then: $R^i \ll R$.

By integrating Eq. 1, the first order kinetic equation can be rewritten as:

$$C(t) = C(0)e^{-kt} \quad (3)$$

Therefore, recovery of the valuable mineral can be calculated by means of the following equation:

$$R = 1 - e^{-kt} \quad (4)$$

According to the Eq. 4, recovery is an exponential function of time. Negative exponential functions become zero in infinity, so the concentration of particles in the kinetic equation never reaches zero, and the recovery approaches a maximum value. This value is called infinite recovery, and by incorporating it in Eq. 4, it would be changed to the following form.

$$R_t = R_\infty(1 - e^{-kt}) \quad (5)$$

Eq. 5 is called standard or classic flotation equation which is the most appropriate and most commonly-used kinetic model [8]. A great number of flotation models have been proposed in order to investigate the flotation kinetic behavior. Solely conventional kinetic models are considered in the scope of this paper (listed in Table 1).

The kinetic study of the flotation process includes obtaining all the parameters which affect the concentrate production rate. Concentrate production can be defined in different ways, but in mineral processing, it is introduced as recovery versus time [9]. By combining the separation time with recovery, two major kinetic curves are produced which are

* Corresponding author. Tel: +98-9123017938, *E-mail address:* a.bahrami@urmia.ac.ir (A. Bahrami).

called process and kinetic curves [13].

Table 1. List of the common kinetic models.

Series No.	Model	Equation	Reference
1	Classic first order model	$R_t = R_\infty(1 - e^{-kt})$	[9]
2	Klimpel model	$R = R_\infty \left\{1 - \frac{1}{kt}(1 - exp\ exp\ (-kt))\right\}$	[10]
3	Fully mixed reactor model	$R = R_\infty \left\{1 - \left(\frac{1}{1 + \frac{t}{k}}\right)\right\}$	[5]
4	Second-order kinetic model	$R = R_\infty \left\{\frac{kt}{1 + kt}\right\}$	[11]
5	Second-order model with rectangular distribution of floatability values	$R = R_\infty \left(1 - \frac{1}{kt}(L_n(1 + kt))\right)$	[12]

In order to obtain the flotation kinetic constant and its influence on the flotation circuits, numerous studies have been conducted. Derzylama et al. (2017) carried out a laboratory scale research on the flotation of different materials and produced some graphs to present the results of the separation process [13]. The separation diagrams included two dimensions with two parameters, one of them was the flotation time. Based on the results of this research, the kinetic constant is derived by integrating the first order kinetic equation.

The present study was conducted to determine the kinetic order and parameters of the flotation process of Gilsonite. Moreover, the particle size distribution of collected clean coal in various flotation stages both in rougher and cleaner processes was analyzed, and six kinetic flotation models were chosen to test their applicability for various size fractions of coal both in rougher and cleaner flotation stages. Additionally, a major objective of the paper was to discuss the differences in the flotation kinetics of various size fractions between rougher and cleaner flotation process.

2. Materials and Methods

2.1. Ore Sample

Asphaltite or Gilsonite is a natural bitumen which consists of complex organic compounds. Gilsonite is a black mineral like obsidian which is brittle and is usually found as brown micronized powder [14]. There are numerous resources of natural bitumen scattered in Iran. The major occurrence of this mineral is in the west and southwest of Iran, and most of them are located in Kermanshah province. The sample investigated in this study was obtained from Geraveh Mine located in Kermanshah province of Iran. According to the mineralogical studies done by a Leitz *SM-LUX-POL* model microscope, in addition to bitumen, sulfur, non-sulfur, and shale particles were detected as impurities (Fig. 1). Silica, shale and silt particles are dispersed in the bitumen background, and the fine cracks are filled with calcite as a secondary mineral. The main tailing materials in the Gilsonite sample are carbonate (calcite and dolomite) and shale compounds, marl, sulfates like gypsum, fine silica, and, opal [15].

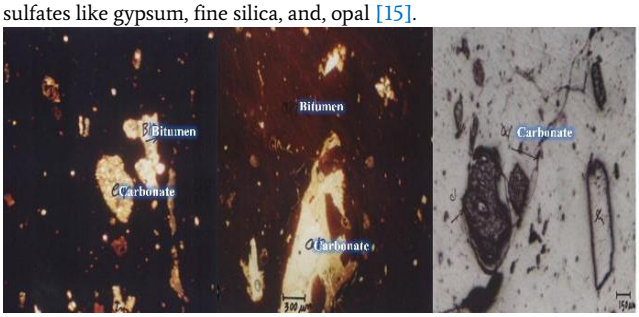

Fig. 1. Photomicrographs of polished sections of Gilsonite sample.

The initial ash content of the sample was determined to be 35%. Results of sieve analysis and the related ash content are listed in Table 2. Also, Table 3 shows the chemical characterization of the Gilsonite sample.

Table 2. Ash content of the Gilsonite sample in each size fraction.

Size fraction (μm)	Mass (%)	Ash content (%)
(-850 , +500)	7.26	-
(-500 , +250)	30.30	34.2
(-250 , +106)	18.75	25.8
(-106 , +75)	13.10	22.2
(-75)	28.96	26.8

2.2. Flotation Tests

The flotation reagents were Gasoline as collector and Pine Oil as frother dissolved in tap water (pH=7.7). The rougher tests were conducted using two reagent combinations: the first trial is the application of Gasoline-Pine Oil combination; and the second is a control test without collector and frother. The rougher tests were performed using pulp density of 10%. Moreover, the concentrate obtained from the former was subjected to a cleaner stage.

Experiments were conducted using a 4.5 *L* Denver *D12* flotation cell with 1800 (*RPM*) agitation rate. In order to perform flotation tests, after preparing the pulp with 10% solid content, collector (concentration: 1750 gr/ton) was added to the cell and mixed for 2 *min*; afterward, frother (300* gr/ton) was also supplemented and mixed for an extra 30 *seconds*. Afterwards, the air valve was opened and frothing was done for 200 *s*. During the operation, the pulp level in the cell was kept constant by replacing the concentrate with tap water.

Table 3. Chemical characterization of the Gilsonite sample.

Volatile matter wt%	Moisture content wt%	Fixed carbon wt%	Specific gravity 25°c	Carbon wt%	Hydrogen wt%	Nitrogen wt%	Oxygen wt%	Sulfur wt%
63	≤3	29	1.11	74	7.1	0.67	3.1	4

The operational parameters of the cleaner experiments were the same as the rougher stage. The final products of the experiments were divided into six parts according to the frothing periods in seconds (0-20), (20-40), (40-60), (60-80), (80-120), and (120-200).

Furthermore, all the products were subjected to sieve analysis using 850, 500, 250, 106, and 75 μm sieves, and all the fractions were weighed and analyzed for their ash content. After obtaining the ash content, the flotation recovery was calculated according to Eq. 6.

$$\%R = \frac{W_c(100 - A_c)}{W_f(100 - A_f)} \times 100 \quad (6)$$

Where, W_c is the concentrate weight, A_c is the ash content of the concentrate and W_f and A_f are the feed weight and the ash content of the feed, respectively.

* The amount of collector and frother has been selected beside on optimum condition.

3. Results and Discussion

3.1. Determination of the Rate of Flotation in Rougher and Cleaner Tests

The results of the Gasoline-Pine Oil test and control tests at the rougher stage were fitted to the models and the associated parameters were calculated according to the classic, Klimpel, fully mixed reactor model, improved gas/solid adsorption model, and rectangular distribution models. Fig. 2 demonstrates that the results of Gasoline-Pine Oil flotation experiment show a high degree of compliance with the all models. Similar findings were also reported by other researchers about the coal [16]. The control test matches the prediction of Second-order kinetic model. In the flotation process, if the grade of the valuable mineral is low or the pulp density is high, kinetic is of the second order [17]. In the control test, less Gilsonite particles were floated and their kinetics followed as the second order model due to the low grade of feed and the lack of collector and frother. The calculated parameters are presented in Table 4.

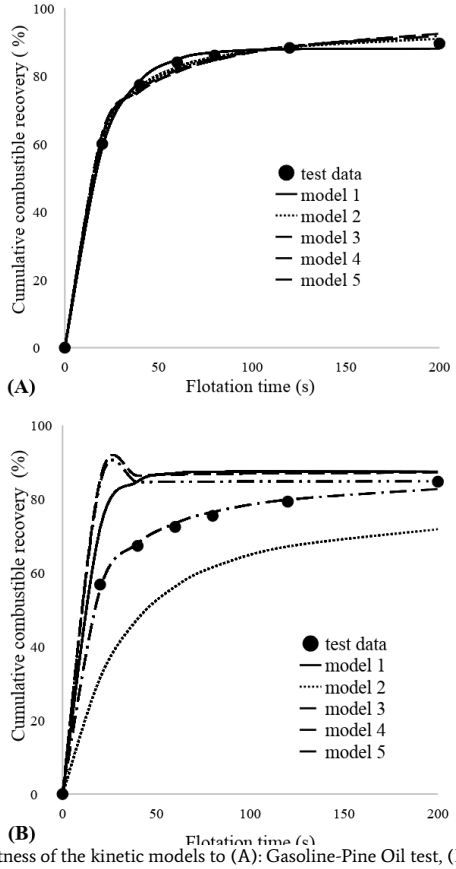

Fig. 2. Fitness of the kinetic models to (A): Gasoline-Pine Oil test, (B): control test rougher flotation tests.

In the rougher flotation experiments using Gasoline-Pine Oil combination, the kinetic constant in the best match with the second order rectangular distribution model is 0.2300 (s^{-1}) and the combustible recovery is 100%. These parameters were obtained to be 0.0869 (s^{-1}), and 87.52%, respectively for the control test. According to Table 4, the final recovery values of the Gasoline-Pine Oil test are higher than the control test with respect to all models. Moreover, the ash content of the flotation concentrates are 23.1 and 26.41%, respectively.

Fig. 3 illustrates the fitness graphs of the combustible recovery-time data for the cleaner experiments. The produced curves indicate that the kinetic of the Gasoline-Pine Oil experiment have a high degree of compliance with the results of all models. Similar results are reported about the coal [16]. Nevertheless, the outcomes of the control test in the cleaner stage correlate with the rectangular distribution model (For reasons mentioned in the rougher flotation, control test). The kinetic constants and combustible recovery of the cleaner tests are 0.0266 (s^{-1}) and 100% for the control tests, respectively. With regard to the Gasoline-Pine Oil test, the kinetic constant in the best match with the second order rectangular distribution model is 0.1589 (s^{-1}) and the combustible recovery is 81.80%. The values of the kinetic parameters related to each kinetic model are presented in Table 4.

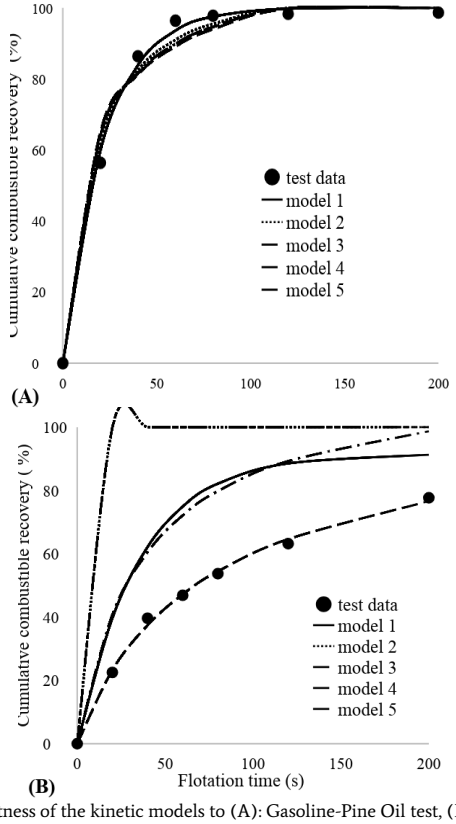

Fig. 3. Fitness of the kinetic models to (A): Gasoline-Pine Oil test, (B): control test cleaner flotation tests.

Table 4. Results of the non-linear regression of the rougher and cleaner data using kinetic models.

Flotation process	Experiments	Model 1			Model 2			Model 3			Model 4			Model 5		
		R_∞	K (s^{-1})	R^2	R_∞	K (s^{-1})	R^2	R_∞	K (s^{-1})	R^2	R_∞	K (s^{-1})	R^2	R_∞	K (s^{-1})	R^2
Rougher stage	Gasoline- Pine Oil	88.03	0.0554	0.9992	94.60	0.1310	0.9994	96.91	11.10	0.9994	96.91	0.0901	0.9994	100.00	0.2300	**0.9995**
	Control test	78.85	0.0563	0.8064	84.92	0.1316	0.6339	87.52	11.50	0.7355	87.52	0.0869	0.9983	91.52	0.2163	**0.6848**
Cleaner stage	Gasoline- Pine Oil	100	0.0454	0.9821	94.16	0.1004	0.9861	94.16	15.157	0.9882	90.68	0.0660	0.9875	81.80	0.1589	**0.9894**
	Control test	61.49	0.0154	0.1982	74.36	0.0284	-	86.01	70.84	-	86.01	0.0141	0.2024	100	0.0266	**0.9976**

As shown in table 4, the amount of combustible recovery is 100% in some cases. R_∞ Is the point in the combustible recovery - time graph where the recovery curve is parallel to the axis of time and recovery returns to a constant value. So in such cases that amounts of recovery were calculated to be greater than 100%, the maximum amount of recovery (100%) was mentioned.

3.2. Effect of Particle Size on the Flotation Kinetic of the Rougher and Cleaner Processes

According to table 4, the combustible recovery of the experiment by using of Gasoline-Pine Oil is higher than the control test according in all models. Therefore, the experiments of Gasoline-Pine Oil were continued to investigate the effect of the particle size on the constant flotation.

The curves of combustible recovery versus flotation time of various size fractions in rougher stage are shown in Fig. 4. As the time passes, the combustible recovery first increases and then approaches a constant value. The highest combustible recovery was achieved in -250+106 µm fraction. It indicated that the maximum combustible recovery was obtained with an intermediate particle size in the rougher flotation process. Similar findings are also reported by other researchers [11, 18, 19].

Flotation is a physio-chemical separation process, in which hydrophobic particles are captured by air bubbles and eventually reported to the froth product. This process is determined by three most critical steps including the particle–bubble collision, attachment, and detachment [19, 11]. It is well known that particle size is an important parameter in flotation process, and a high process efficiency of froth flotation is typically limited to a relatively narrow particle size range [20]. However, outside this range, the recovery drops significantly, whether it is at the fine or the coarse end of the size spectrum [21]. The low combustible recovery of fine particles is mainly due to the poor collision and attachment between the fine particles and air bubbles, whereas the poor combustible recovery of coarse particles is primarily related to the high probability of detachment between the coarse heavy particles and air bubbles [17, 21, 22].

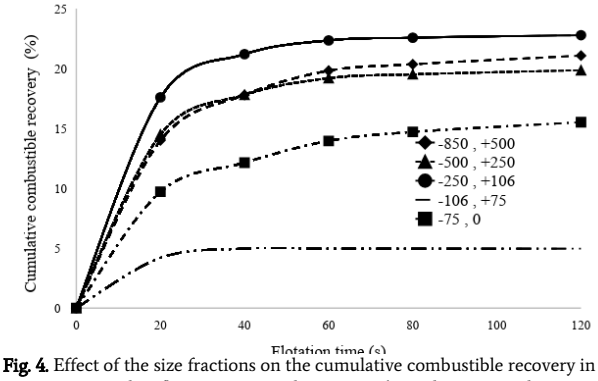

Fig. 4. Effect of the size fractions on the cumulative combustible recovery in the rougher flotation process by means of Gasoline-Pine Oil.

The cumulative combustible recovery values at 20, 40, 60, 80, 120, and 200 *seconds* with various size fractions in rougher flotation process were fitted to five flotation kinetic models (Table 1) using MATLAB. Furthermore, the values of the flotation constant, the maximum combustible recovery, and correlation coefficient of each model were calculated and presented in Table 5. The maximum values of combustible recovery for all models increases by the particle size decrease. This trend continues to the -250+106 µm fraction, then decreases for -106+75 µm and elevates again for the -75 µm size fraction. The difference in kinetics constants (both K and R_∞) of various size fractions can be justified by the combined effect of the collision and attachment/detachment sub-processes in flotation process [23, 24].

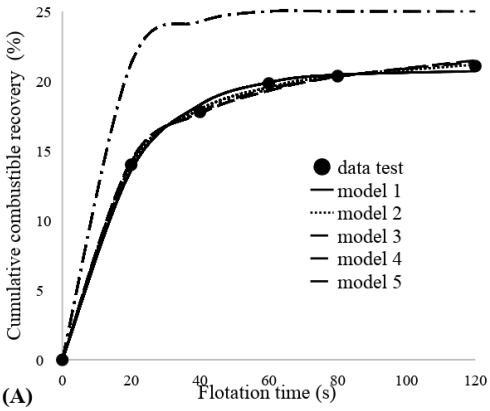

(A)

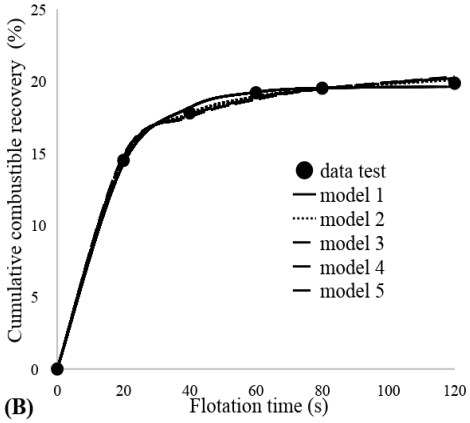

(B)

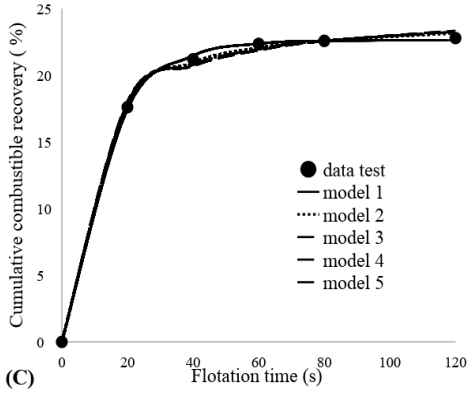

(C)

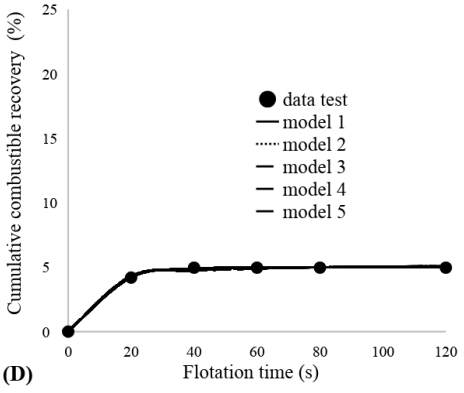

(D)

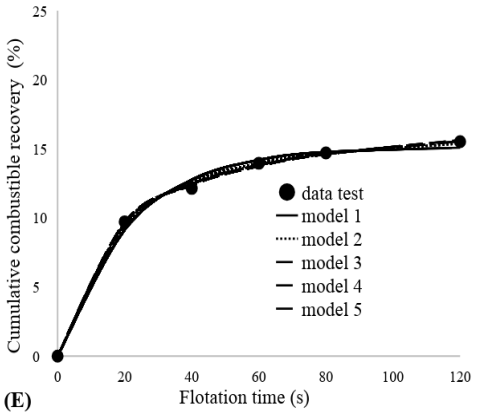

Fig. 5. Fitting kinetic models on the data derived from different size fractions in rougher flotation (A): (-850+500); (B): (-500+250); (C): (-250+106); (D): (-106+75); (E): (-75) µm.

Fig. 3 shows the flotation time-combustible recovery of various size fractions in the cleaner stage of flotation. Maximum combustible recovery for different size fractions in the cleaner stage was related to the -850+500 µm. Given that the particle range fraction is also an significant factor in recovery results, it can be inferred that in -850+500 µm fraction, Gilsonite particles have the best type of fracture (spherical), and the feed in this particle size and shape results in the best separation. In other words, the connection of particles to air bubbles is better and the recovery will be higher. The results of the multi-variate nonlinear regression in the cleaner flotation stage for the applicable size fraction were presented in Fig. 7 and Table 5.

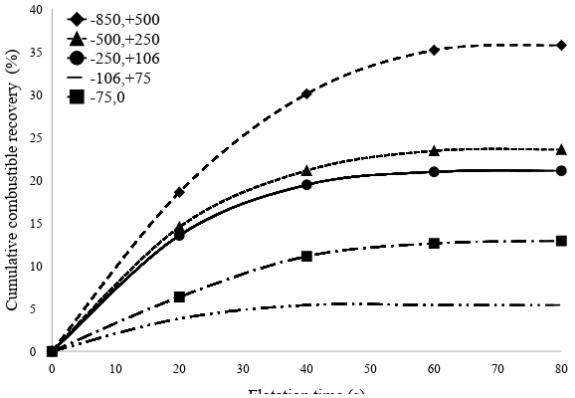

Fig. 6. Effect of the size fraction range on the cumulative combustible recovery in the cleaner flotation process by means of Gasoline-Pine Oil.

In the cleaner stage, each size fraction correlates with a different kinetic model and in contrast to the rougher tests, the combustible recovery declines with the particle size. This trend continues until -106+75 µm fraction and then ascends.

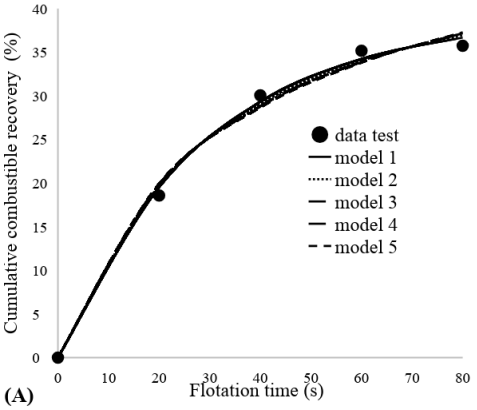

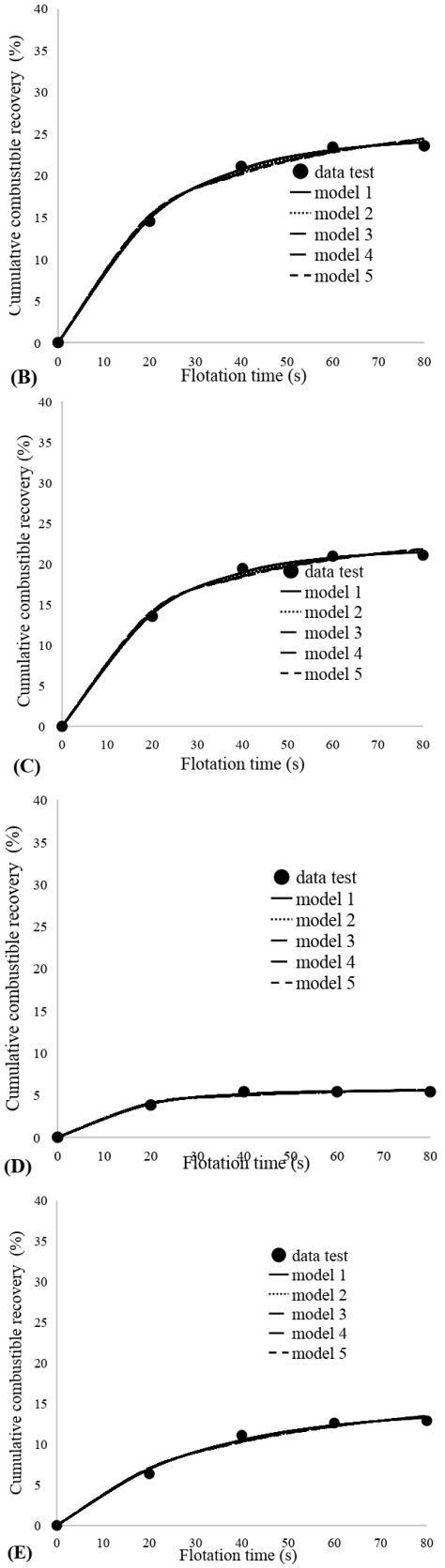

Fig. 7. Fitting kinetic models on the data related to different size fractions in cleaner flotation stage (A): (-850+500); (B): (-500+250); (C): (-250+106); (D): (-106+75); (E): (-75) µm.

Table 5. Results of the nonlinear regression of the rougher and cleaner data using kinetic models.

Flotation process	Size fraction of particles *(μm)*	Model 1			Model 2			Model 3			Model 4			Model 5		
		R_∞	K (s^{-1})	R^2	R_∞	K (s^{-1})	R^2	R_∞	K (s^{-1})	R^2	R_∞	K (s^{-1})	R^2	R_∞	K (s^{-1})	R^2
Rougher stage	-850+500	20.74	0.0535	0.9988	22.81	0.1166	0.9998	23.79	13.566	0.9996	23.79	0.0737	0.7390	25.27	0.1710	0.9993
	-500+250	19.63	0.0651	0.9994	21.26	0.1516	0.9997	21.85	9.656	0.9993	21.85	0.1036	0.9993	22.87	0.2594	0.9999
	-250+106	22.63	0.0740	0.9998	24.25	0.1826	0.9994	24.72	7.571	0.9990	24.72	0.1321	0.9990	25.64	0.3513	0.9987
	-106+75	4.99	0.0933	0.9995	5.24	0.2715	0.9977	5.27	4.505	0.9972	5.27	0.2220	0.9972	5.38	0.6817	0.9968
	<75	15.14	0.0462	0.9963	16.80	0.0978	0.9991	17.73	17.045	0.9996	17.75	0.0587	0.9996	19.07	0.1298	0.9997
Cleaner stage	-850+500	39.13	0.0346	0.9984	46.24	0.0617	0.9985	52.37	32.719	0.9986	52.37	0.0306	0.9986	59.54	0.0577	0.9984
	-500+250	24.58	0.0646	0.9992	28.19	0.0888	0.9987	30.57	20.335	0.9984	30.57	0.0492	0.9984	33.64	0.1009	0.9986
	-250+106	21.83	0.0506	0.9990	24.83	0.0990	0.9984	26.62	17.585	0.9980	26.62	0.0569	0.9980	29.03	0.1200	0.9981
	-106+75	5.57	0.0632	0.9963	6.20	0.1302	0.9952	6.48	12.100	0.9946	6.48	0.0826	0.9946	6.91	0.1895	0.9950
	<75	14.27	0.0333	0.9967	16.96	0.0586	0.9974	19.38	35.093	0.9977	19.38	0.0285	0.9977	22.16	0.0531	0.9983

As shown in Fig. 4 and 6, the slope of the curves for various size fractions in the cleaner flotation stage is steeper than those of the rougher flotation stage. Furthermore, the cumulative combustible recovery of various size fractions demonstrates little change after 120 *seconds* in the rougher stage but the similar time in the cleaner stage was 80 s.

4. Conclusion

In this research, the differences in flotation rate were studied for Gilsonite for various size fractions between rougher and cleaner stages. According to the experimental results, data from rougher and cleaner stages using Gasoline-Pine Oil combination, shows a high degree of compliance with the prediction of all models (R^2>0.999). On the other hand, the results from the rougher and cleaner experiments without reagents correlated well with the models of Modified Gas/Solid Adsorption, and Rectangular Distribution with k values of 0.0869 (s^{-1}), and 0.0266 (s^{-1}), respectively. With regard to test with Gasoline-Pine Oil as reagents, the kinetic constant in the best match with the second order Rectangular Distribution Model is 0.2300 (s^{-1}) and the combustible recovery is 92.4739%. In all of the first order kinetic models, the maximum recovery values were related to the tests with Gasoline-Pine Oil.

When the effect of particle size on the combustible recovery and flotation rate in the rougher and cleaner stages is concerned, the maximum combustible recovery was associated with the size fractions of -250+106 μm in the rougher experiments; and maximum combustible recovery was related to the -850+500 μm fraction in the cleaner tests while using Gasoline-Pine Oil reagents combination. For both rougher and cleaner flotation stages, the kinetic constant increases with decreasing particle size until the size fraction of -106+75 μm, and afterwards the value of k decreases.

REFERENCES

[1] Agar, G. E., & Barrett, J. J. (1983). The use of flotation rate data to evaluate reagents. *CIM. Bulletion 76 (851)*, 157-162.

[2] Urbina, R. H. (2003). Recent developments and advances in formulations and applications of chemical reagents used in froth flotation. *Mineral Processing and Extractive Metallurgy Review 24(2),* 139-182. https://doi.org/10.1080/08827500306898.

[3] Garcia-Zuniga, H. (1935). Flotation recovery is an exponential function of time. *Bulletin Minero de la Societal National de Minero*, Santiago, Chile.

[4] Tomlinson, H. S., & Fleming, M. G. (1963). Flotation rate studies. *6th International Mineral Processing Congress, Cannes*, 563-579.

[5] Imaizumi, T., Inoue, T. (1963). Kinetic considerations of froth flotation. *6th International Mineral Processing Congress, Cannes*, 581-593.

[6] Lynch, A. J., Johnson, N. W., Manlapig, E. V., & Thorne, C. G. (1981). Mineral and coal flotation circuits, their simulation and control. *Elsevier Scientific Publishing Company.*

[7] Lazic, P., & Calic, N. (2000). Boltzman's model of flotation kinetics. *Proc. XXI IMPC (Rome),* B8a, 87-93.

[8] Oliveira, J. F., Saraiva, S. M., Pimenta, J. S., & Oliveira, A. P. A. (2001). Kinetics of pyrochlore flotation from Araxa mineral deposits. *Miner. Eng. 14 (1),* 99–105. https://doi.org/10.1016/S0892-6875(00)00163-1.

[9] EK, C. (1992). Flotation kinetics. *Innovation in flotation technology*, Canada: 183-210. https://doi.org/10.1007/978-94-011-2658-8_8.

[10] Klimpel, R. R. (1980). Select ion of chemical reagents for flotation, Mineral Processing Plant Design. *AIME,* 907-934.

[11] Zhang, H., Liu, J., Cao, Y., & Wang, Y. (2013). Effects of particle size on lignite reverse flotation kinetics in the presence of sodium chloride, *Powder Techno, 246*, 658–663. https://doi.org/10.1016/j.powtec.2013.06.033.

[12] Trahar, W. J., & Warren, L. J. (1976). The floatability of very fine particles-a review. *Int. J. Miner. Process* 3, 103–131. https://doi.org/10.1016/0301-7516(76)90029-6.

[13] Drzymala, J., Ratajczak, T., & Kowalczuk, P. (2017). Kinetic separation curves based on process rate considerations. *Physicochemical problems of mineral processing 53(2)*, 983-995. http://hdl.handle.net/11250/2464431.

[14] Helms, J., Kong, X., Salmon, E., & Hatcher, P. (2012). Structural characterization of Gilsonite bitumen by advance nuclear magnetic resonance spectroscopy and ultrahigh resolution mass spectrometry revealing Pyrrolic and aromatic rings substituted with aliphatic chains. *J. of organic Geochemistry, Elsevier 44*, 21-36. https://doi.org/10.1016/j.orggeochem.2011.12.001.

[15] Kazemi, F. (2017). Site Selection of Gilsonite ore Dressing Plant, Based on Industrial Specification of Mine (Kermanshah), *Master of Science Thesis in Mining Engineering*, Faculty of Engineering-urmia University, (In Persian).

[16] Ni, C., Xie, G., Jin, M., Peng, Y., & Xia, W. (2016). The difference in flotation kinetics of various size fractions of bituminous coal between rougher and cleaner flotation processes. *Powder Technology 292*, 210–216. https://doi.org/10.1016/j.powtec.2016.02.004.

[17] Mehrotra, S. P., & Kapur, P. C. (1974). The effects of aeration rate, particle size and pulp density on the flotation rate distributions. *Powder Technol. 9(74),* 213–219. https://doi.org/10.1016/0032-5910 (74)80044-6

[18] Tao, D. (2005). Role of bubble size in flotation of coarse and fine particles-a review. *Sep. Sci. Techno 39 (4)*, 741–760. http://dx.doi.org/10.1081/SS-120028444.

[19] Muganda, S., Zanin, M., & Grano, S. R. (2011). Benchmarking flotation performance: single minerals. *Int. J. Miner. Process 98 (3–4)*, 182–194. https://doi.org/10.1016/j.minpro.2010.12.001.

[20] Shahbazi, B., Rezai, B., & Javad Koleini, S. M. (2010). Bubble–particle collision and attachment probability on fine particles flotation. *Chem. Eng. Process. Process Intensify 49(6)*, 622–627. https://doi.org/10.1016/j.cep.2010.04.009.

[21] Jameson, G. J. (2010). Advances in fine and coarse particle flotation. *Can. Metall. Q 49 (4)*, 325–330. https://doi.org/10.1179/cmq.2010.49.4.325.

[22] Schubert, H. (2008). On the optimization of hydrodynamics in fine particle flotation. *Miner. Eng. 21 (12–14)*, 930–936. https://doi.org/10.1016/j.mineng.2008.02.012.

[23] Abkhoshka, E., Kor, M., & Rezai, B. (2010). A study on the effect of particle size on coal flotation kinetics using fuzzy logic. *Expert Systems with Applications 37 (7)*, 5201–5207. https://doi.org/10.1016/j.eswa.2009.12.071.

[24] Li, Y., Zhao, W., Gui, X., & Zhang, X. (2013). Flotation kinetics and separation selectivity of coal size fractions. *Physicochemical. Problem. Min. Process 49 (2)*, 387–395.